Endmembers, Pixel Unmixing, and Clustering.

David B. Reister[1], Jerry C. Ritchie[2], and Albert Rango[3]

[1]Oak Ridge National Laboratory, Oak Ridge, TN 37831-6355
[2]USDA ARS Hydrology and Remote Sensing Laboratory, Beltsville, MD 20705
[3]USDA ARS Jornada Experimental Range, Las Cruces, NM 88003

Abstract

A new clustering algorithm for unsupervised classification has been developed. The algorithm has been applied to a hyperspectral field data set (with information classes) and the resulting spectral classes are consistent with the information classes. ENVI has two clustering algorithms for unsupervised classification: Isodata and K-means. For our data set, the clusters found by both Isodata and K-means were significantly different than our clusters. Further analysis found that both Isodata and K-means placed about half of the measurements in the wrong cluster.

I. INTRODUCTION

Endmembers have been used to analyze multispectral and hyperspectral images since the paper by Adams, *et al.* [1] that analyzed an image of Mars using four image endmembers, that included a shade endmember. The three nonshade image endmembers were identified by comparison with a library of laboratory reflectance spectra. The measured spectrum (ρ_i) of a pixel in the image is the weighted average of the spectra of the endmembers (a_{ij}) and the weights (p_j) are the fraction of the total area of the image that is occupied by each subcomponent:

$$\rho_i = \sum_j a_{ij} p_j \ , \tag{1}$$

where the weights are nonnegative numbers that sum to one.

Gillespie, et al. [2] analyzed hyperspectral AVIRIS (Airborne Visible/Infrared Imaging Spectrometer) data using image endmembers. The number of endmembers is one more than the numerical rank (K) of the measurements, which can be determined by using Principal Component Analysis (PCA) to find the number of dimensions required to explain the data variance. However, PCA does not identify the endmembers, which are extreme pixels in data clusters. Boardman and Goetz [3] estimated an illumination factor at each pixel and constrained the weights to be nonnegative and to sum to one or less. Boardman [4] uses the framework of the geometry of convex sets to identify the K+1 end members as the vertices of the smallest simplex that bounds the measured data. Roberts, *et al.* [5] have developed multiple endmember spectral mixture analysis, in which they evaluated 889 two-endmember models and used the evaluation results to generate 276 three-endmember models. The best 24 two-endmember and 12 three-endmember models were chosen to generate vegetation maps.

Boardman and Roberts are using endmembers in quite different ways. Boardman generates a single set of endmembers and calculates the weights for each pixel to determine the fractional abundance patterns in the region. Roberts has a large library of laboratory and field measurements and evaluates many

two-endmember models. Since a two-member model has one free parameter, he finds which model provides the best fit for each pixel. However, the results are not unique and one or more of the models may provide a good fit for a pixel.

Our objective is the same as Boardman and Roberts: to group hyperspectral measurements into as many distinct classes as possible. Richards and Jia [6] draw the distinction between information classes and spectral classes, where information classes are human classifications and spectral classes are groups or clusters of measurements made by a computer.

We will consider (1) to be a general linear mixing model and allow the spectra and weighs to be any real number. The spectra are columns of the matrix $\boldsymbol{A}$. All linear combinations of the spectra form a subspace (the range space of $\boldsymbol{A}$) that has a numerical rank (K) and can have many sets of basis vectors. The null space of $\boldsymbol{A}^{\mathrm{T}}$ is all vectors that are orthogonal to $\boldsymbol{A}^{\mathrm{T}}$.

We distinguish between two problems: forward and inverse. For the forward problem, we are given the spectra of the subcomponents and the weights, and we calculate the measured spectra. For the inverse problem, we are given the spectra of the subcomponents and the measured spectra, and we calculate the weights. While the forward problem always has a unique solution, the inverse problem usually does not have a unique solution. Given a solution to the inverse problem, another solution can be found by adding any vector from the null space of $\boldsymbol{A}^{\mathrm{T}}$.

Since pixel unmixing is an inverse problem, there should be many solutions to the pixel unmixing problem. The basic problem is that the measured spectra are not linearly independent, but are highly correlated. Singular value decomposition (SVD) [7] can be used to create an uncorrelated orthonormal basis for the spectra, that will provide a solution to the inverse problem. The solution for the inverse problem could also be expressed as a linear combination of any K linearly independent members of the original spectral library. However, this form of pixel unmixing is neither unique nor informative.

In Section II, we will describe a method for partitioning hyperspectral measurements into distinct classes. When we began our research, we expected that the distinct classes would be a basis for the measurements. As the research has progressed, we realized that the basis vectors are not classes. Instead, the classes are groups (clusters) of distinct measurements. There can be many more classes than there are basis vectors. A familiar example is the population distribution on the Earth's surface. We know that there are many distinct towns and cities on the 2D surface of the Earth.

Section III will discuss the methods used to collect a hyperspectral field data set at the Jornada Experimental Range near Las Cruces, NM. In Section IV, we will use our clustering method to partition the field measurements into distinct groups and compare the clusters (spectral classes) with the labels (information classes) that were given to each of the field measurements at the time of data collection. The final section presents our conclusions.

II. CLUSTERING ALGORITHM

Hyperspectral sensors measure radiance and the data can be transformed to reflectance. For each of N spatial measurements, we transform the data by subtracting the mean of the M spectral values and normalizing to unit length. After the transformation, the data [a_{ij}, where i = 1, M and j = 1, N] have the following properties:

$$\sum_i a_{ij} = 0 \ . \tag{2}$$

$$\sum_i a_{ij}^2 = 1 \tag{3}$$

The components of the correlation matrix (c_{jk}) are defined by:

$$c_{jk} = \sum_i a_{ij}\, a_{ik} \ . \tag{4}$$

The Euclidean distance (d_{jk}) between two measurements is defined by:

$$d_{jk} = \sum_i \left(a_{ij} - a_{ik}\right)^2 . \tag{5}$$

Using (3) and (4), the Euclidean distance is directly related to the components of the correlation matrix

$$d_{jk} = 2\left(1 - c_{jk}\right) . \tag{6}$$

We will define the cluster radius (r_c) by:

$$r_c = \mathbf{max}\left[1 - c_{jk}\right] . \tag{7}$$

Our clustering algorithm depends on two parameters, the cluster radius (r_c) and the minimum number of members in a cluster (n_c). For each value of the cluster radius, we define the set of spectral neighbors (ψ_k) for each spatial measurement point:

$$\psi_k = \left\{ j \mid j \in [1, N], c_{jk} > 1 - r_c \right\} \tag{8}$$

Since the limits on the correlation coefficient are ± 1, the cluster radius will be in the interval [0,2]. For a sufficiently small cluster radius, all of the neighborhoods (ψ_k) will have one member (the point k). For a sufficiently large cluster radius, all of the neighborhoods will have all N points.

The first cluster is the neighborhood with the most members. Each subsequent cluster is the neighborhood with the most members that are currently not part of any of the clusters. We stop adding clusters, when the neighborhood with the most members has fewer than n_c members. We use our clustering method to partition measurements into the maximum number of distinct groups. Although the maximum number of groups will occur with one measurement in each group (n_c = 1), we want to have several members in each neighborhood (n_c > 1). If we were prospecting for rare mineral deposits, we might cluster most of the measurements and then prospect in the neighborhoods that had the most unclustered members. For a fixed value of n_c, we vary the cluster radius to find the maximum number of clusters. For small values of the radius, there will not be any clusters. For large values of the radius, there will be one cluster. For some intermediate value of the radius, there will the maximum number of clusters.

Each cluster is the neighborhood of a measurement, which we shall call the root vector and use to represent the typical vector in the cluster. Alternative ways of choosing a typical vector (that require more computation) are to calculate the mean value or to use SVD to calculate the first basis vector for the cluster.

III. HYPERSPECTRAL FIELD MEASUREMENTS

The United States Department of Agriculture (USDA) Agricultural Research Service (ARS) Jornada Experimental Range (Jornada) in southern New Mexico has a long history of research, experimentation, and monitoring [8] making it a unique location to study the effect of climate change on the interface between desert grassland and desert shrub ecosystems and to test different remote sensing techniques and systems for monitoring and detecting these changes. The Jornada Experimental Range was established in 1912 under the jurisdiction of the USDA Bureau of Plant Industry. In 1915 the USDA Forest Service assumed control at Jornada and began collecting climate and vegetation data. Some research plots and data records have been maintained since 1912 [9]. The management of Jornada was transferred from the Forest Service to the Agricultural Research Service in 1954. In 1977, the site was selected as a Biosphere Reserve as part of the United Nations International Man and the Biosphere program. In 1981 the National Science Foundation selected Jornada as a Long-Term Ecological Research (LTER) site. These different programs and research efforts at Jornada have produced a 91-year history of long-term ecological research on processes related to vegetation change, desertification, and range management. These historic and ongoing investigations have produced a wealth of ground data on vegetation characteristics, ecosystem dynamics, and vegetation responses to hydrologic, atmospheric, and human inputs [10].

In 1995, the Jornada Experiment (JORNEX) was begun by ARS investigators to periodically collect data from ground, airborne, and satellite-based remote sensing platforms at three dominant vegetation communities (Grass, Transition, and Mesquite) along 150 m long vegetation transects. Beginning in 1997, hyperspectral plant canopy and soil reflectance measurements have been collected twice a year at Jornada using an Analytical Spectral Devices (ASD)[1] full-range (350 – 2500 nm) spectrometer [10]. These data were obtained on a 30x30 m grid at 5 m intervals and at 5-m intervals along 150-m vegetation transects. Separate radiometric measurements were made for each frequently encountered plant species, litter, and base soil (10 measurements of each selected cover type). Measurements are made in Spring and Fall to coincide with the overpass of Landsat and Terra/Aqua satellites. ASD measurements are recorded as digital values and converted to radiance based on instrument calibration and to reflectance by comparison with measurements from a standard white reflectance panel.

In September 2000, 665 ASD field measurements were made at the Jornada at three dominant vegetation communities . We analyzed only the 211 measurements that were made at the grass site for this paper. Each measurement consists of 2151 numbers that are the reflectance values at wavelengths ranging from 350 nm to 2500 nm in 1 nm steps. Each measurement is described with one or two of the following 12 labels: "Bare", "Litter", "Aristida", "Capa", "Datu", "Forb", "Grass", "Mesquite", "Senna", "Snakeweed", "Tila", and "Yucca". Here, "Bare" represents bare soil, "Litter" represents

---

1 Trade names are included for the benefit of the reader and do not imply an endorsement of or a preference for the product listed by the ORNL or the U. S. Department of Agriculture.

plant litter, and the other 10 labels designate plant species (Table 1). These labels provide an information classification for the measurements.

Label	Description-Plant Name	Common Name	Type
Bare	Bare soil with no litter or vegetation		
Litter	Soil covered with organic litter		
Grass	Multiple species of grass		
Forb	Multiple species of herbaceous plants		
Aristida	*Aristida purpurea* Nutt.	Purple threeawn	Perennial grass
Capa	*Croton pottsii* (Klotzsch) Mull. Arg.	Leather weed	Annual forb
Datu	*Dasyochloa pulchella* (Kunth) Willd. ex Rydb.	Fluff Grass	Perennial grass
Mesquite	*Prosopis glandulosa* Torr.	Honey mesquite	Perennial shrub
Senna	*Cassia bauhinioides* A. Gray	Two-leaf senna	Perennial shrub
Snakeweed	*Gutierrezia sarothrae* (Pursh) Britton & Rusby	Broom snakeweed	Perennial sub-shrub
Tila	*Tidestromia lanuginosa* (Nutt.) Standl.	Espanta vaquero	Annual forb
Yucca	*Yucca elata* Engelm.	Soap-tree yucca	Perennial shrub

Table 1. Description of vegetation and soils.

IV. HYPERSPECTRAL DATA ANALYSIS

Using SVD, we calculated an orthonormal basis for the 211 measurements and calculated the coordinates of each vector using the basis. The basis vectors are the principal axis of the hyperellipsoid that bounds the measurements. The first basis vector is the mean value for the 211 measurements; the second and higher components are the directions with the most variance in the data. The first basis vector explains 82.63 % of the variance, the first four vectors capture 99.33% of the variance, the first eight vectors capture 99.78% of the variance, and the first fifteen vectors capture 99.90% of the variance. We will define the numerical rank (K) by determining the number of basis vectors required to explain 99% of the variance in the data. Thus, K is 4 for this data set.

To demonstrate how the SVD basis captures the variance in the data, we will examine several 2D "slices" through a subset of the 4D set of points. The first coordinate represents the correlation between the measurement and the mean value for all of the measurements. Since most of the correlations are greater than 0.95 the first coordinate is not very useful for separating the measurements into groups. A plot of the second coordinate vs the third coordinate for four of the labels is shown in Fig. 1. There is a group representing mixed "Bare" and "Litter" in the lower right quadrant of the plot. Most of the "Grass" measurements are in the upper left quadrant; the "Grass" measurements are not as tightly clustered as measurements for "Bare" and "Litter" categories. The "Forb" measurements range from the lower left quadrant to the upper right quadrant and overlap with the "Grass" measurements. Since the "Grass" and "Forb" are labels for collections of multiple species, it is not surprising that measurements are not tightly clustered. There is a clean separation between the "Bare" and "Litter" group and the "Grass" and "Forb" group.

The second 2D "slice" is a plot of a3 vs a4 (Fig. 2). The fourth coordinate provides good separation between the "Bare" and "Litter" measurements, and reasonably good separation of the "Forb" and

"Grass" measurements. Thus, the fourth coordinate separates groups that overlapped in Fig. 1. The two graphs illustrate that the measurements for the four information classes are in four different regions of the spectral space.

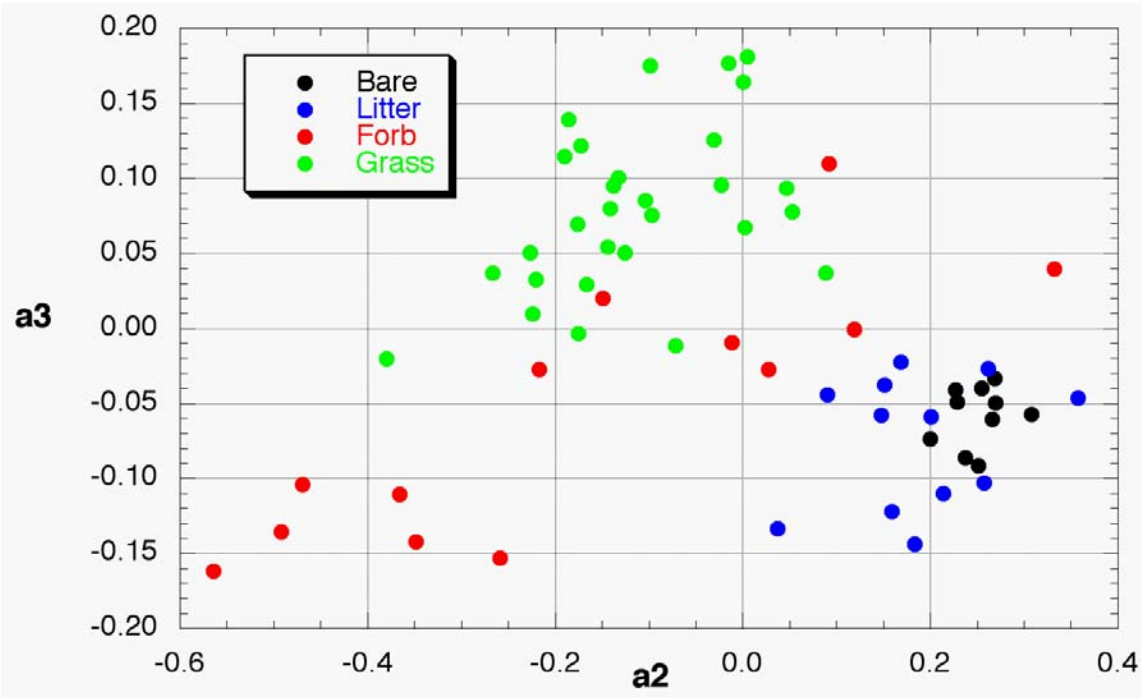

Fig. 1. Plot of the second coordinate (a2) vs the third coordinate (a3) for four groups of measurements.

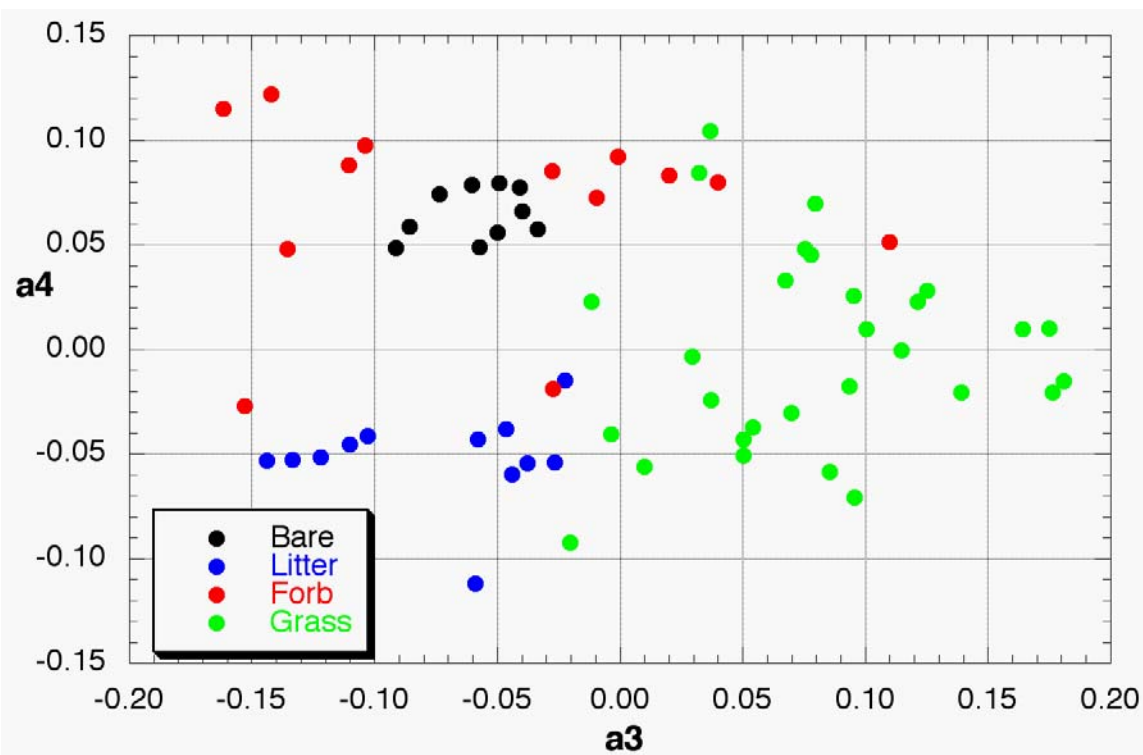

Fig. 2. Plot of the third coordinate (a3) vs the fourth coordinate (a4) for four groups of measurements.

Our clustering method has two parameters: the cluster radius (r_c) and the minimum number of members in a cluster (n_c). We chose n_c to be 4 and we vary r_c to find the maximum number of clusters. A plot of the number of clusters for several values of r_c is shown in Fig. 3. The maximum number of clusters is 20; this maximum occurs for a cluster radius of 0.007 (the correlation coefficients then are >0.993 for each cluster). As the radius increases, the number of unclustered vectors that remain, after all of the clusters have been chosen, decreases monotonically. With this clustering technique and data set, the number of unclustered vectors is 55 when the number of clusters is 20.

The clusters are chosen to have the largest possible number of unclustered vectors, but they can also include vectors that are members of other clusters. For the data that we examined, only 5 of the 20 clusters include vectors that are members of other clusters (Fig. 4). Our clustering method revealed 20 (almost) distinct spectral classes that could be labeled and become information classes.

The members of each of the clusters are summarized in Table 2. Each cluster consists of the neighbors of a measurement vector that has a label. The label for the first cluster is "Grass/Bare", and the members of the first cluster are primarily "Grass" and "Bare". In all 20 cases, the label of the root measurement in the cluster is consistent with the cluster membership. For cluster 18, the members are 50% "Snakeweed" and 50% "Mesquite", and the root measurement is "Snakeweed". All of the 12 labels are at the root of at least one of the clusters.

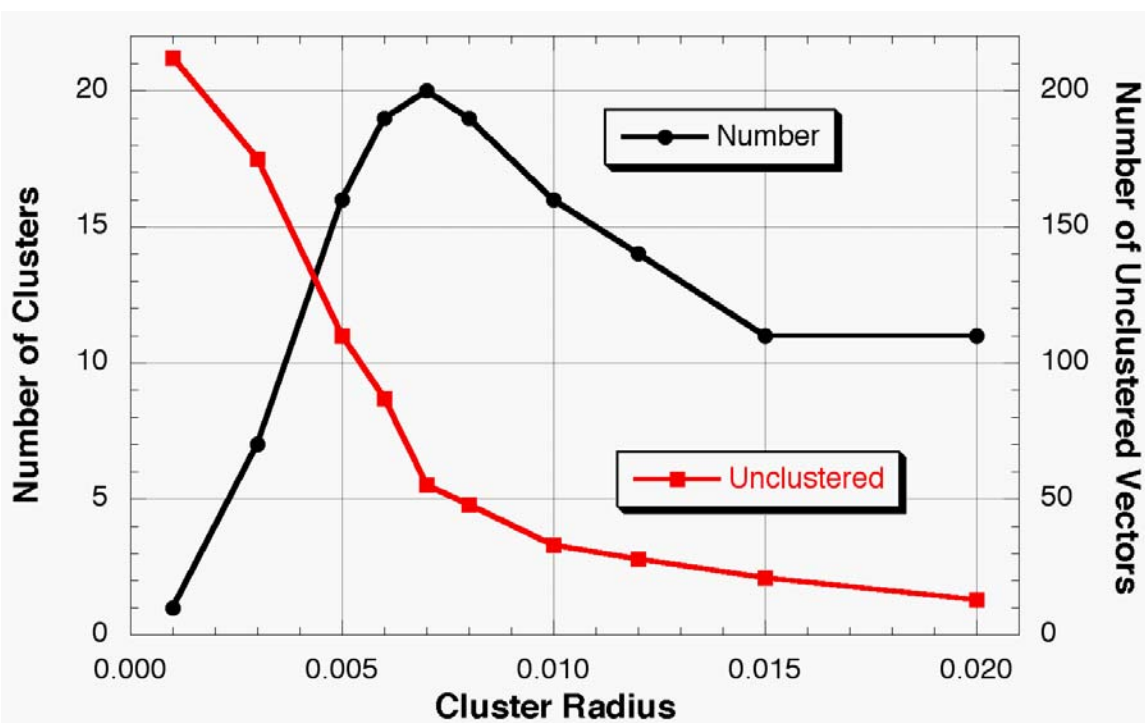

Fig. 3. Number of clusters and unclustered vectors versus the cluster radius.

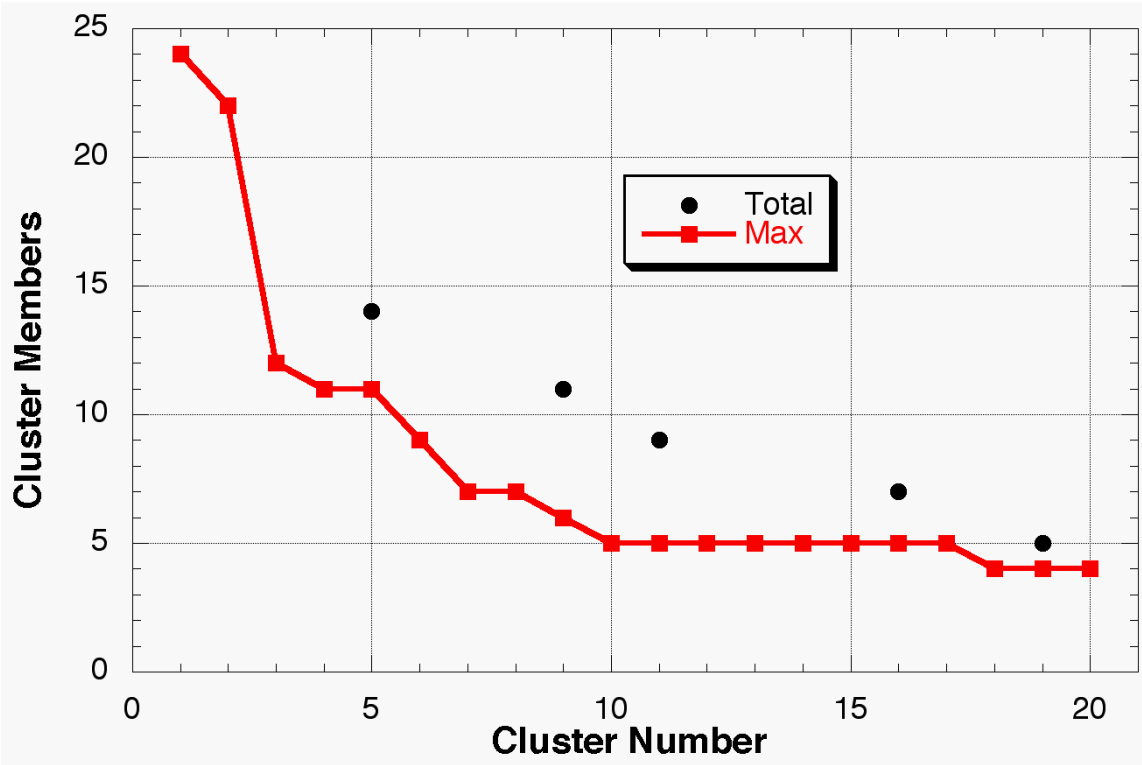

Fig. 4. Number of unclustered vectors in each cluster (Max) and the total number of vectors in each cluster (Total).

Using the SVD orthonormal basis, we can plot the location of the 20 root vectors on 2D "slices" through a 5D space. We begin with a plot of Axis 1 vs Axis 2 (Fig. 5). Axis 1 is not useful for distinguishing distinct groups in the 12 root vectors that have more than a 0.95 correlation with axis 1. However, it is quite useful for the 8 root vectors that have lower correlations with axis 1. The two measurements with the lowest values are both "Yucca" (a1 = 30% and 22%). The next two measurements are both "Mesquite" (a1 = 61% and 83%). The next four values are: "Tila" (85%), "Aristada" (86%), "Snakeweed" (90%), and "Senna" (93%). Axis 2 begins to separate the 12 measurements with a1 above 95%.

Figs 6, 7, and 8 show plots for Axis 2 vs Axis 3, Axis 4, and Axis 5, respectively. These three plots can be used to see which axis of the orthonormal basis will separate one root measurement from another. The measurements with a2 greater than –45% that were touching or overlapping in Fig. 5 are revealed distinctly in Fig. 6. Similarly, two root vectors with overlapping values of a2 (-45.3% and –45.7%) have distinct values for a3 (-9.5% and –22.9%). The three measurements that have the highest values in a2 are overlapping in Fig. 5, but quite distinct in the next three Figs (see Table 3).

Cluster	Bare	Litter	Grass	Forb	Datu	Snake	Capa	Senna	Arist	Tila	Mesq	Yucca
1	29	13	46	8			4					
2	9		77	9			5					
3												100
4	95	5										
5	11		14	11	7	7	29	14		7		
6					11		22	56	11			
7			64	7		29						
8												100
9	41	23		18								
10	50	10	40									
11			89			11						
12				40							60	
13											100	
14									100			
15								20		80		
16					72		14	14				
17		100										
18						50					50	
19	10		30	60								
20									100			

Table 2. The membership (percent) of each cluster.

Label	a1 (%)	a2 (%)	a3 (%)	a4 (%)	a5 (%)
Grass/Litter	95.9	24.7	12.4	3.9	-0.7
Bare	96.1	25.1	-9.1	4.8	-2.6
Litter	96.0	26.2	-2.7	-5.3	5.5

Table 3. Coordinates for three measurements that overlap in a1 and a2, but which have distinct values for a3, a4, and a5.

When discussing Fig. 5, we noted that 12 root vectors were highly correlated with the mean vector and 8 root vectors were less correlated. We will call these two groups: central clusters and outlier clusters and their normalized reflectance is plotted in Figs. 9 and 10.

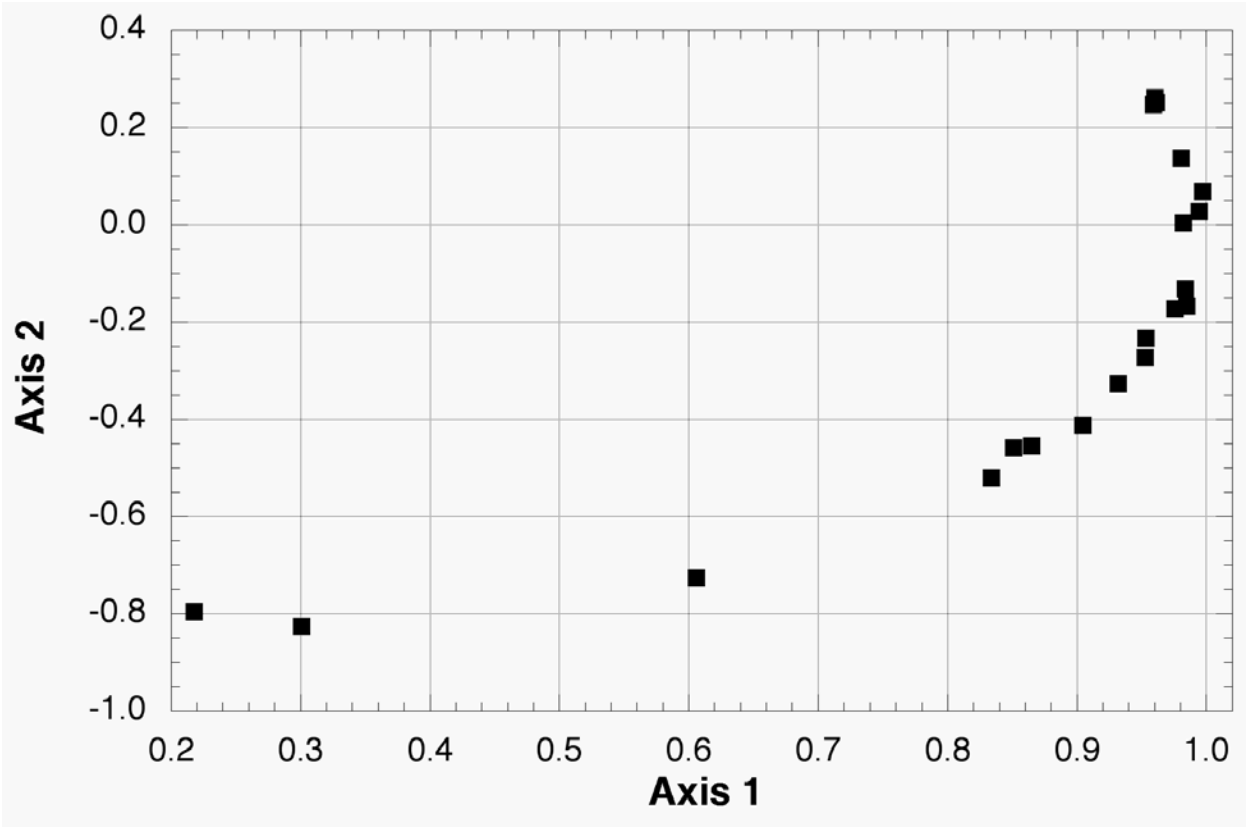

Fig. 5. The location of the 20 root vectors on Axis 1 vs Axis 2.

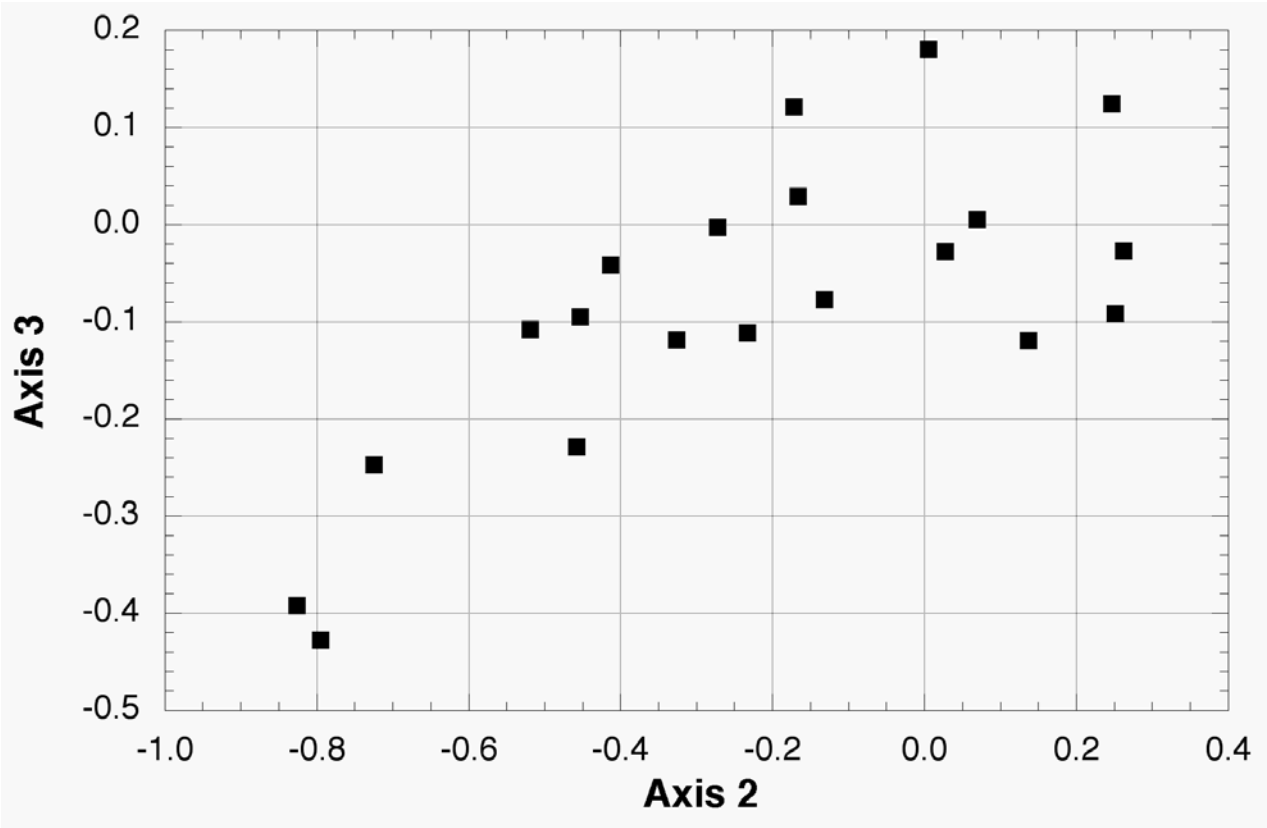

Fig. 6. The location of the 20 root vectors on Axis 2 vs Axis 3.

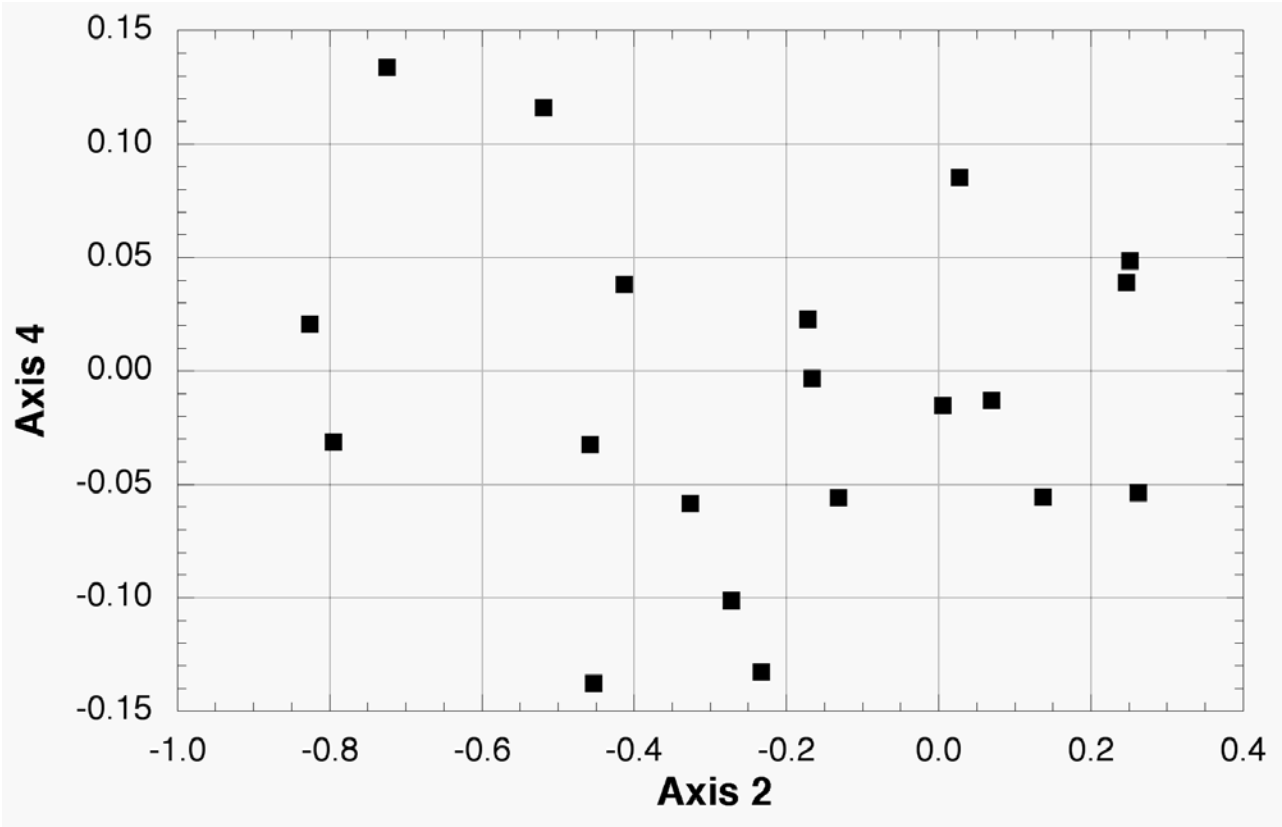

Fig. 7. The location of the 20 root vectors on Axis 2 vs Axis 4.

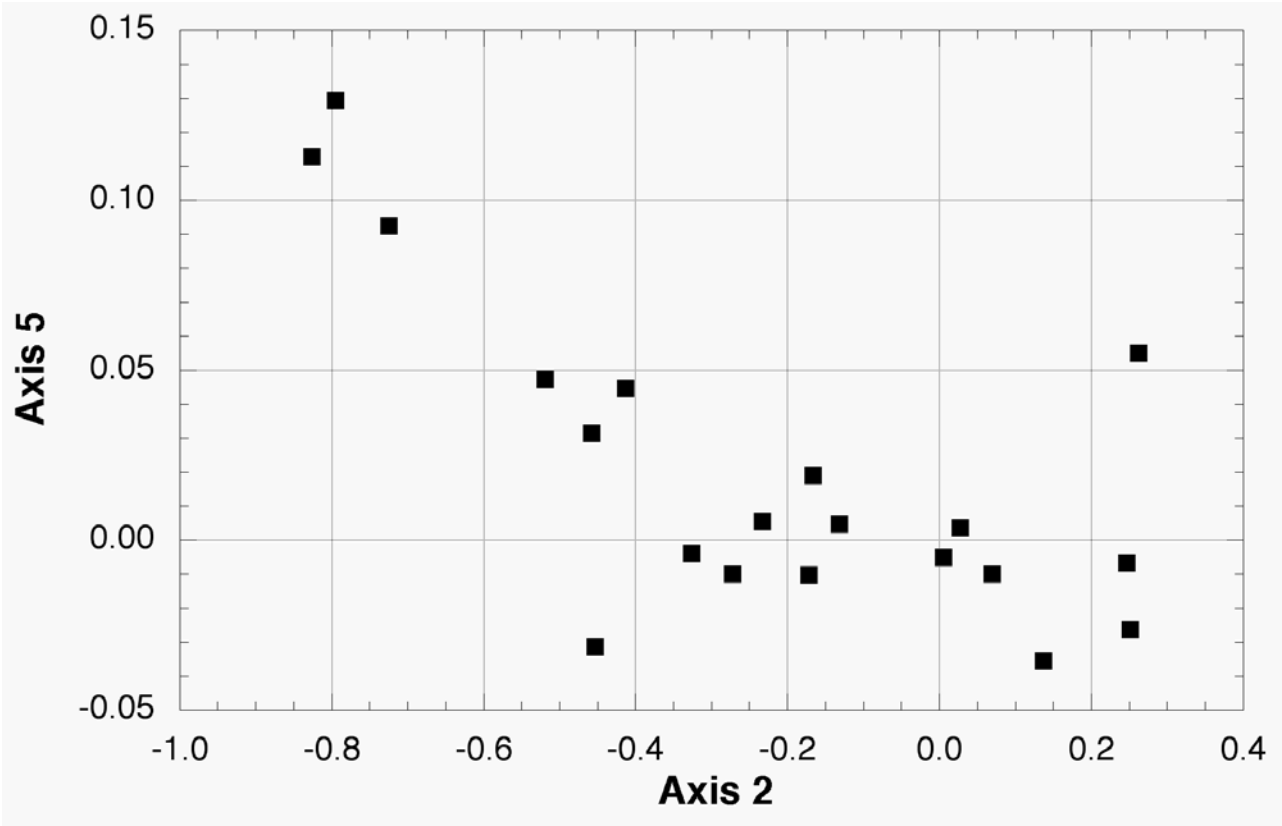

Fig. 8. The location of the 20 root vectors on Axis 2 vs Axis 5.

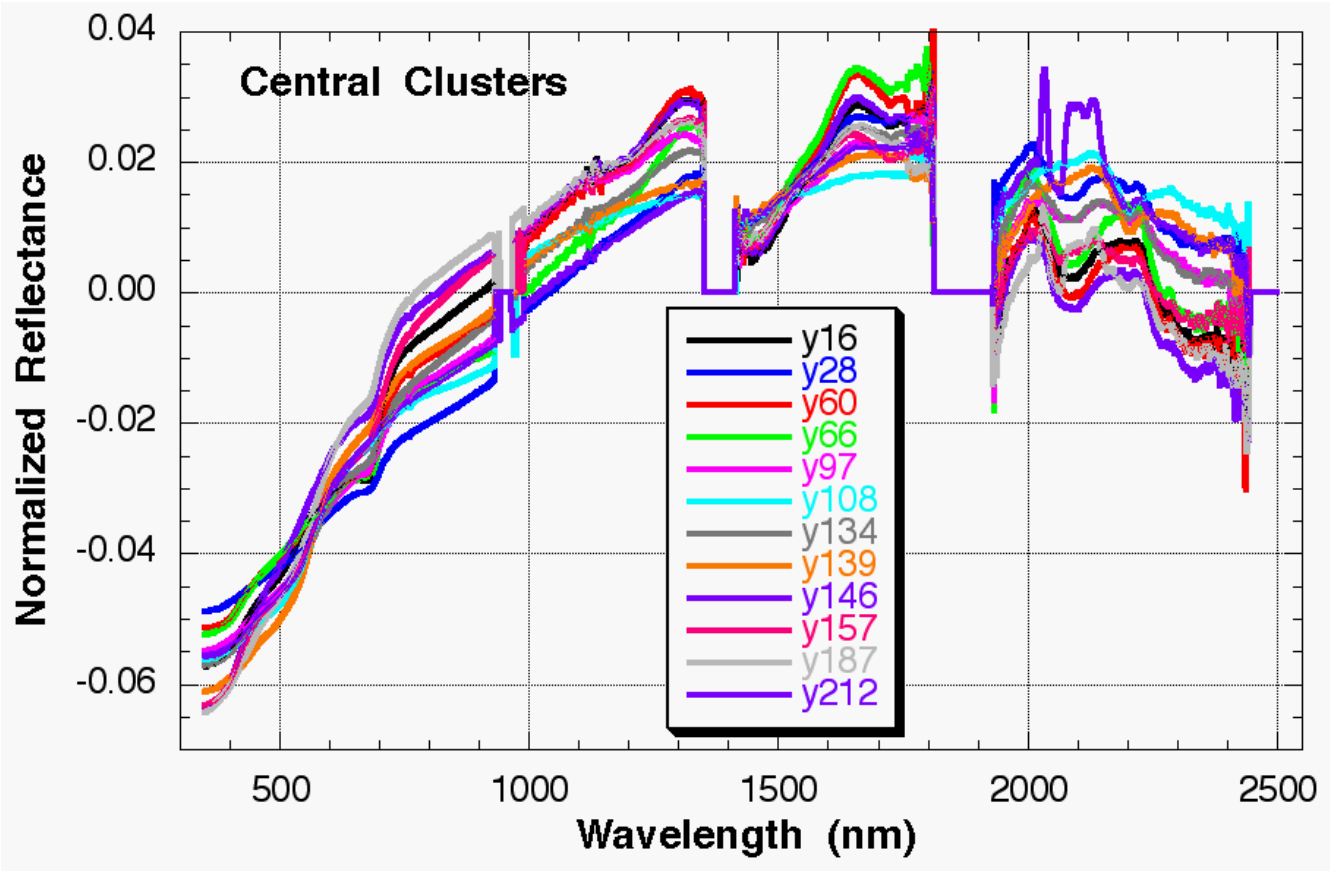

Fig. 9. Normalized reflectance for the central clusters.

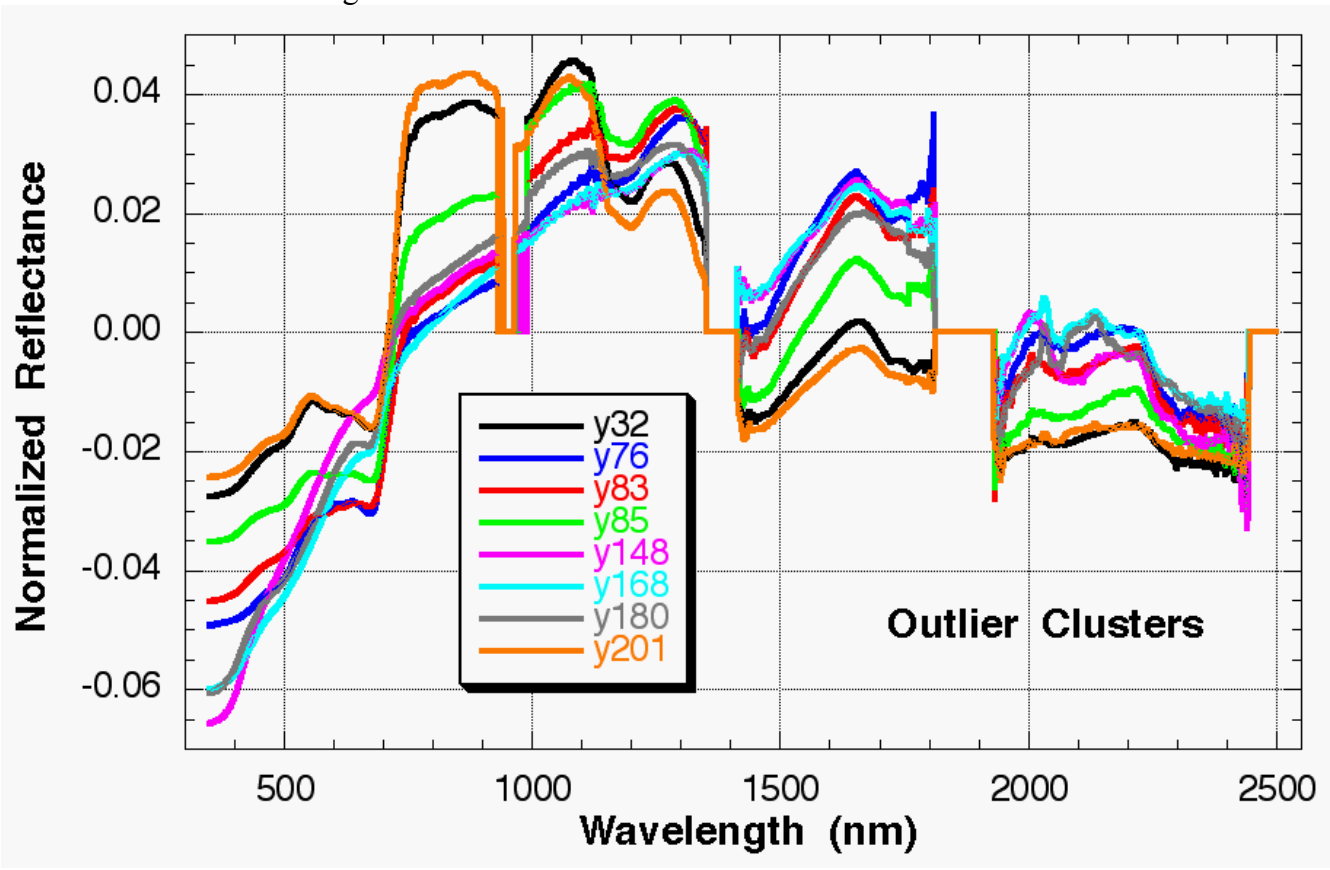

Fig. 10. Normalized reflectance for the outlier clusters.

V. OTHER CLUSTERING METHODS

ENVI is a software package that is widely used for processing hyperspectral data. ENVI has two clustering methods: Isodata and K-Means. For both clustering methods, the user chooses the number of clusters (m_c). The initial step is to choose m_c measurements as the cluster centers. Both methods iterate on the following two steps. 1. Assign each of the N measurements to the cluster whose cluster center is closest to it (using the Euclidean distance norm). 2. For each cluster, the new cluster center is the mean value of the measurements in the cluster. The iterations stop when the changes in cluster membership are sufficiently small. The Isodata method includes merging clusters if they are too small and splitting clusters that are too large. The ENVI versions of the two methods include several other options. For both methods, the user can specify the maximum standard deviation from the mean and/or the maximum allowable distance error.

We used both Isodata and K-means to analyze our data set and compared the resulting clusters to our clusters. When we found significant differences, we analyzed the reasons for the discrepancy. Both Isodata and K-means define clusters by providing the cluster number for each measurement. Given the cluster members, the mean value for each cluster can be used to calculate the distance between the mean and each member. The cluster radius [defined by (7)] is the largest distance for the cluster members. We found that the most of the cluster radii were much larger than the radius for our method (0.007) (see Fig. 3). When a cluster has a large radius, many members of other clusters can be inside the ball defined by the radius and we will call all of the points inside the ball: neighbors. Members and neighbors are plotted in Fig. 12 for the Isodata case and in Fig. 13 for the K-means case.

To reduce the cluster radii, we adjusted the maximum allowable distance error. Although we reduced the radius, the number of neighbors remained high. When we calculated which cluster center was closest to each measurement, we were surprised to find that more than half of the measurements (112 of 211 for the Isodata case and 115 for the K-means case) were in the wrong cluster! If the software errors in ENVI were corrected, many of the cluster radii would be reduced. There are also some cases where a measurement is in the correct cluster, but it is much farther away from the cluster center than the other members. In this case, the cluster should be split, with a new cluster center for the outlier.

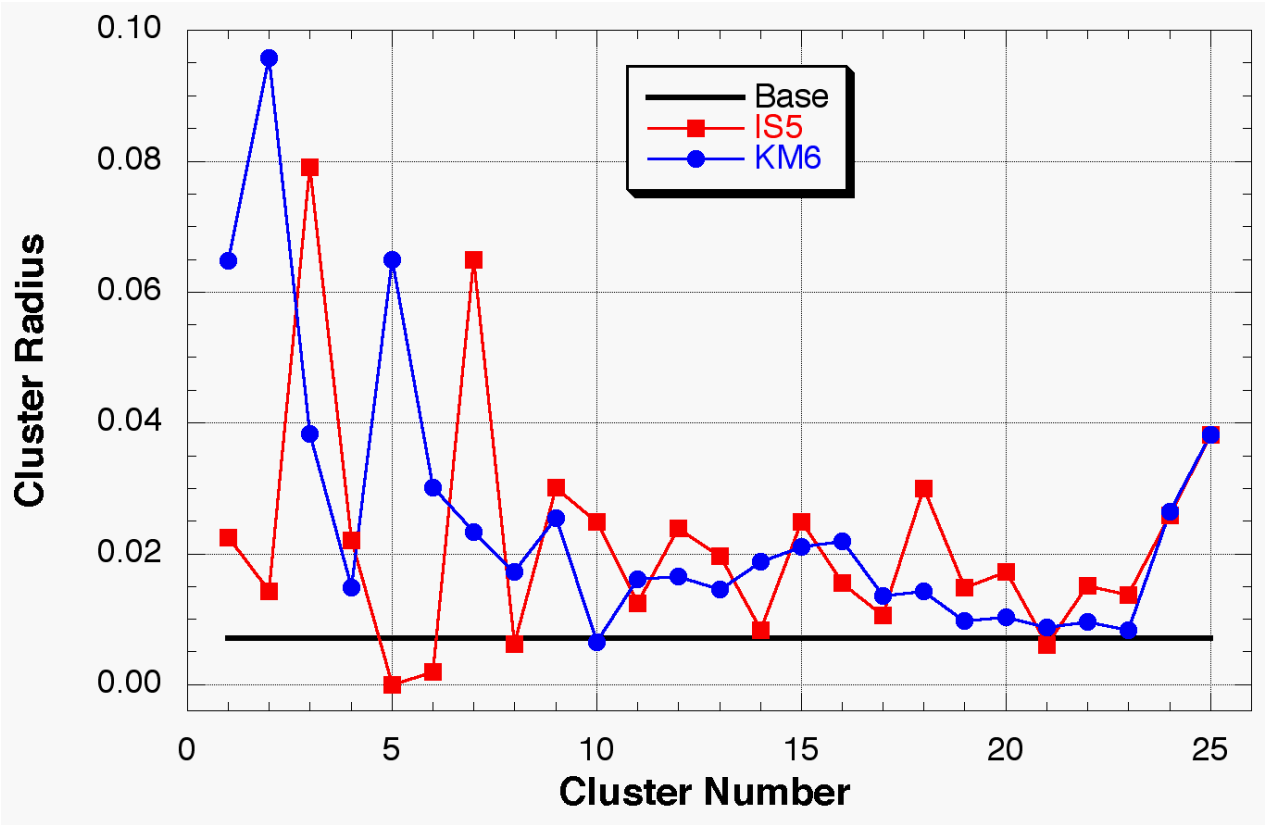

Fig. 11. The cluster radii for the Isodata (IS5) and the K-means (KM6) clusters compared to our base value (0.007).

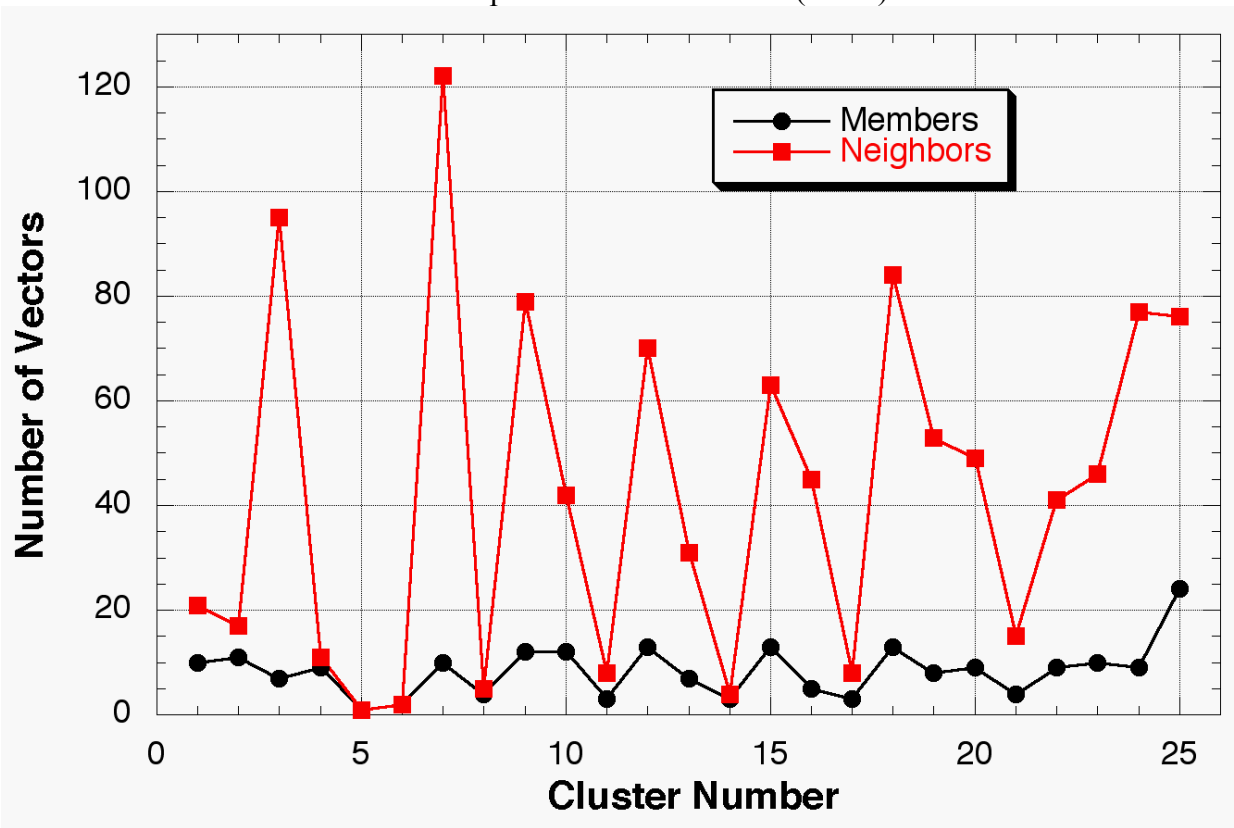

Fig. 12. Members and neighbors for the Isodata (IS5) case.

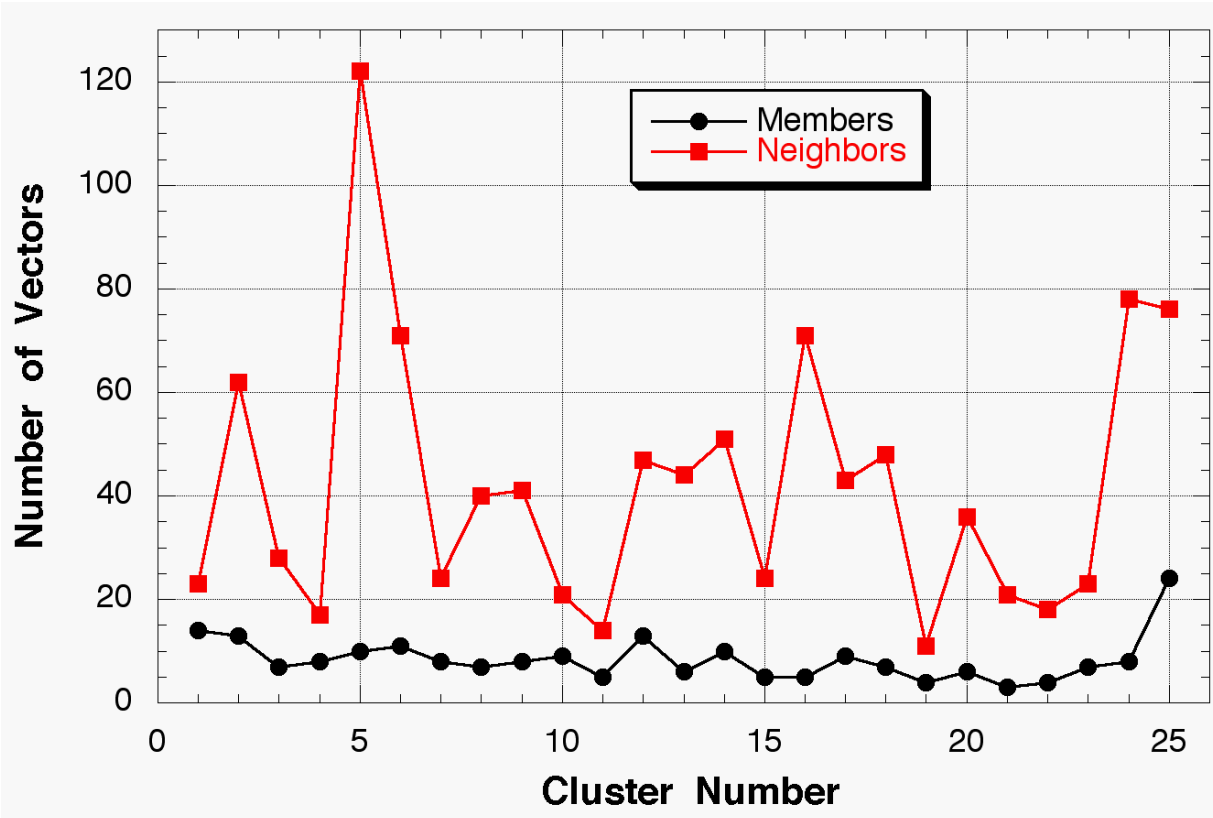

Fig. 13. Members and neighbors for the K-means (KM6) case.

Our clustering method requires less computation than the Isodata and K-means methods when there are many clusters. The major computation is to calculate the distance between each measurement and every cluster center. Each time the cluster members change, the mean value must be recalculated and the distance calculation must be repeated. For our method, we only need to calculate the distance between each pair of measurements once.

VI. DISCUSSION AND CONCLUSIONS

Our objective is to group hyperspectral measurements into as many distinct classes as possible. A new clustering algorithm for unsupervised classification has been developed. The algorithm has been applied to a hyperspectral field data set (with information classes). Using SVD, we calculated an orthonormal basis for the 211 measurements. When we define the numerical rank (K) as the number of basis vectors required to explain 99% of the variance in the data, we find that K = 4 for this data set.

In our clustering algorithm, we vary the cluster radius to find the maximum number of clusters. For this data set, the maximum number of clusters is 20. Each cluster consists of the neighbors of a root measurement vector that has a label. In all 20 cases, the label of the root measurement in the cluster is consistent with the cluster membership. All of the 12 labels are at the root of at least one of the clusters.

Using the first five vectors in the SVD basis for the measurements, we have plotted the location of the 20 root vectors on 2D "slices" through a 5D space. While axis 1 is not useful for distinguishing distinct groups in the central clusters (the 12 root vectors that have more than a 0.95 correlation with axis 1), it is quite useful for separating the central clusters from the outlier clusters (the 8 root vectors that have

lower correlations with axis 1). The slices reveal that each of the 12 root vectors for the central clusters has a distinct location in the 5D space.

ENVI has two clustering algorithms for unsupervised classification: Isodata and K-means. For our data set, the clusters found by both Isodata and K-means were significantly different than our clusters. We found that the most of the cluster radii were much larger than our radius and the largest radius was more than a factor of 10 larger. When a cluster has a large radius, many members of other clusters can be inside the ball defined by the radius. Further analysis found that both Isodata and K-means placed more than half of the measurements in the wrong cluster. Since our algorithm does not require iterations, it requires less computation for large data sets than Isodata and K-means. Thus, our new algorithm appears to advance the state-of-the-art.

ACKNOWLEDGMENT

This research was supported by the U. S. Department of Energy (DOE) Office of Fossil Energy (Office of Natural Gas and Petroleum Technology) through the National Petroleum Technology Office and the DOE Office of Science (Office of Basic Energy Sciences). ORNL is managed by UT-Battelle, LLC for the U. S. Department of Energy under Contract No. DE-AC05-00OR22725.

REFERENCES

1. J. B. Adams, M. O. Smith, and P. E. Johnson, "Spectral mixture modeling: A new analysis of rock and soil types at the Viking Lander 1 site", *J. Geophys. Res*., vol. 91, no. B8, pp. 8098-8112, 1986.

2. A. R. Gillespie, M. O. Smith, J. B. Adams, S. C. Willis, A. F. Fischer III, and D. E. Sabol. "Interpretation of residual images: Spectral mixture analysis of AVIRIS images, Owens Valley, California", *AVIRIS Workshop Proc.*, JPL Publication 90-54, Jet Propulsion Laboratory, Pasadena, CA, pp. 243-270, 1990.

3. J. W. Boardman and A. F. H. Goetz, "Sedimentary facies analysis using AVIRIS data: A geophysical inverse problem", *AVIRIS Workshop Proc.*, JPL Publication 91-28, Jet Propulsion Laboratory, Pasadena, CA, pp. 4-13, 1991.

4. J. W. Boardman, "Automated spectral unmixing of AVIRIS data using convex geometry concepts", *AVIRIS Workshop Proc.*, JPL Publication 93-26, Jet Propulsion Laboratory, Pasadena, CA, pp.11-14 (1993).

5. D. A. Roberts, M. Gardner, R. Church, S. Ustin, G. Scheer, and R. O. Green, "Mapping chaparral in the Santa Monica mountains Using multiple endmember spectral mixture models", *Remote Sens. Environ.,* vol. 65, no. 3, pp. 267-279, 1998.

6. J. A. Richards and X. Jia, "Remote Sensing Digital Image Analysis", Third Edition, Springer-Verlag, Berlin (1999).

7. G. H. Golub and C. F. Van Loan, "Matrix Computations",3rd ed., Baltimore, MD, The Johns Hopkins University Press, 1996.

8. F.N. Ares, "The Jornada Experimental Range: An Epoch in an Era of Southwestern Range Management", Range Monograph No. 1, Society for Range Management, Denver, CO, 74pp, 1974.

9. K. Havstad and W. Schlesinger, “Reflections on a century of rangeland research in the Jornada Basin of New Mexico”. In Proceedings of Shrubland Ecosystem Dynamics in a Changing Environment(J.R. Barrow, E.D. McArthur, R.E. Sosebee, and R.J. Tausch, Eds.), USDA Forest Service, General Technical Report, INT-GTR-338, 10-15, 1966.

10. K. M. Havstad, W. P. Kustas, A. Rango, J. C. Ritchie, and T. J. Schmugge, "Jornada Experimental Range: A unique arid land location for experiments to validate satellite systems", *Remote Sen. Environ*., vol. 74, no. 1, pp. 13-25, 2000.